*16th World Conference on Earthquake, 16WCEE 2017*

*Santiago Chile, January 9th to 13th 2017*

*Paper N° 1071*

*Registration Code: S-D1463057249*

# ADAPTING EMPIRICAL MMI FORMULAE AIMED AT DEVELOPING EARLY TSUNAMI HAZARD ASSESSMENT CHARTS

J. L. Baquedano [(1)], P. A. Catalán [(2,3)], Y. Hayashi[(4)]

*[(1)]Msc. Student, Dept. de Obras Civiles, Univ. Técnica Federico Santa María, jose.baquedano@alumnos.usm.cl*
*[(2)]Associate Professor, Dept. de Obras Civiles, Univ. Técnica Federico Santa María, patricio.catalan@usm.cl*
*[(3)]Associate Researcher, CIGIDEN*
*[(4)]Senior Researcher, Seismology and Tsunami Research Dept., Meteorological Research Institute, Japan, yhayashi@mri-jma.go.jp*

## *Abstract*

In recent years, Chile has been exposed to an important number of strong earthquakes that have triggered tsunamis of different amplitudes and extension. Notable examples include the Maule earthquake (Mw 8.8) which took place on February 27th, 2010; the Iquique earthquake (Mw 8.1) on April 1st, 2014; and the Illapel earthquake (Mw 8.3) on September 16th, 2015. These events have permitted to identify some weaknesses of the then existing Chilean Tsunami Warning system, and to devise an improvement strategy that has been implemented recently. Despite these improvements, due to the information flow procedure and time required to process data, there is still some uncertainty regarding the exact area potentially affected by a tsunami immediately after an earthquake occurs, and, more importantly, a finite time before solutions are found. Hence the necessity of a faster, but reliable first assessment of hazard, defined with low level parameters.

In this paper, an analysis of the relation between the intensity of an earthquake (via the Modified Mercalli Intensity, MMI) and the occurrence of a tsunami and its expected wave height is performed, taking into account the distance from the point of interest to the hypocenter, and the earthquake magnitude. The objective of this is to test whether the Mercalli Intensity Scale can be used as a tool which adds support to the existing system from a technical point of view, during the period of when no other data driven technical assessments are available.

First, a series of empirical formulae relating the intensity with either Peak Ground Acceleration or Peak Ground Velocity, and others that relate PGA or PGV with the parameters that define the earthquake (e.g. depth, magnitude, dip, and strike, among others) are tested and calibrated to the Chilean case. To perform this, data available from earthquakes occurred between 2011 and 2014 are used. In order to verify and validate the results obtained, additional data from 2015 earthquakes are utilized. The result is an empirical relationship between MMI, hypocentral distance and earthquake magnitude.

Next, to obtain the corresponding tsunami hazard, numerical simulations of a range of scenarios are performed to ensure data coverage and statistical robustness. Here, a series of points of interest located around nine coastal cities are considered to create city-specific charts which relate tsunami hazard with MMI curves as well. A city-specific approach is used under the premise that a tsunami would vary greatly among different locations, even under the same conditions, due to bathymetric and topographic controls.

By completing the aforementioned steps, an additional and fast way to evaluate the risk of a tsunami after a considerably large seismic event will be available for use and, in consequence, the current evaluation system could be reinforced; thereby improving its reliability and the area over which a preventive evacuation alert could be issued.

*Keywords: Tsunami Forecast Chart; Empirical Relation Assessment; Spatial Tsunami Variability; Scenario Propagation.*

## 1. Introduction

The worldwide state of the art of tsunami warning systems (TWS) points towards a tsunami energy measurement [1], in order to effectively capture its potential damage along the coast. This is an evolution from the original alert systems in Japan which estimated tsunami characteristics based solely on the parameters of the preceding earthquake, which lead in some cases to misleading predictions, causing both over and underestimations of the tsunami devastating power.

Nowadays, the Chilean TWS is managed by three different and independent entities. The *Centro Sismológico Nacional* (CSN) provides the basic information about the earthquakes that have occurred in the national territory (e.g. epicenter coordinates, time of occurrence, magnitude, among other data), which is to be sent to the *Oficina Nacional de Emergencia del Ministerio del Interior y Seguridad Pública* (ONEMI) and to the *Servicio Hidrográfico y Oceanográfico de la Armada de Chile* (SHOA). The latter is responsible to evaluate and determine the tsunami hazard, informing back to ONEMI, which finally defines the need to evacuate a certain area after an earthquake [2]. However, in the intervening time between an earthquake and the first, data based, tsunami hazard assessment, the protocol relies heavily on how the earthquake was felt, characterized by intensity reports collected and issued by ONEMI personnel scattered along the country. This period of time is long enough for the procedure to consider triggering preventive evacuation if a Modified Mercalli Intensity (MMI) of VII, or above, are reported. It must be noted that as a result, an evacuation can be implemented based on subjective data alone and also might involve a large part of the territory. Erroneous assessments could happen due to the subjective nature of the Mercalli Intensity. The most notable example of this potential problem is an earthquake occurred on August 23rd, 2014 (Mw 6.4), when an Intensity of VII was reported in Talca, which is roughly 300 kilometers south of the epicenter, while in Valparaíso, located just 40 km south of it, an Intensity of VI was reported. Fortunately, no evacuation was put in place. However, what this example shows is that there are weaknesses in the current protocols that in other cases could potentially be inadequate. Hence the necessity of an improved use of the MMI, which, despite its possible subjectivity, can be quite useful, when no other data are available

To this end, our aim is to provide a more robust way to estimate the likelihood of a tsunami occurrence in the period when no instrumental data are available. This work is loosely based on previous tsunami forecast charts (TFC) used until 1999 in Japan, with two main differences. The first corresponds to the use of the Modified Mercalli Intensity (MMI) as a starting point in the evaluation of the potential tsunami hazard on the corresponding TFC. The second is that the TFCs to be created are location specific. Different TFCs are to be built for different cities, in contraposition to the Japanese chart, which is unique nationwide.

The main hypothesis for the work is that it is possible to use MMI to develop a system of curves which relate MMI to the magnitude of the earthquake, and the distance, from the point of evaluation to the hypocenter. Moreover, it is possible to couple these curves to the potential tsunami hazard, which is also dependent on magnitude and hypocentral distance. As a result, an evaluation relying on the MMI can be performed.

With this in mind, the main objectives are two. In first place, analyze the usage of the MMI as a forecast tool. This is done via the creation of charts relating MMI with magnitude and distance, by recurring to existing empirical models, available data, and a new model. And secondly, to build tsunami forecast charts for nine coastal cities along the country as a way to demonstrate site effects can be relevant. The end results are city-specific TFCs which can be used as a quick tsunami forecast tool.

## 2. Methodology

### 2.1 MMI-Δ-Mw curves

The first step is to determine the relationship between the Modified Mercalli Intensity, hypocentral distance, and moment magnitude. To this end, raw data of available reports spread along the Chilean coast (from 2011 to 2014) are classified by MMI and Mw. Events where the epicenter is inland away from the coast, or reported data from non-coastal cities, are discarded.

One of the relevant parameters is the minimum hypocentral distance, defined as the distance from the point of interest to the closest point belonging to the fault plane of the earthquake. This distance is calculated by a simplified model that takes into consideration both the dimensions of the fault plane and whether the projection of the point of interest falls or not into the fault plane, whose dimensions are estimated from the scaling laws of Papazachos et al. (2004) [3]. Values of dip and strike of each associated fault plane are taken from the Global Centroid-Moment-Tensor (CMT) website. When the earthquake has a magnitude smaller than 6.7 the dimensions of the rupture are negligible, so the hypocentral distance is simply estimated as the hypotenuse of the triangle formed by the epicentral distance and the focus depth. There are recorded routinely by ONEMI and CSN at the moment of the event. Hence, for each event a vector consisting of MMI, Mw and hypocentral distance is constructed.

For each set of MMI, a preliminary relationship between Mw and hypocentral distances is obtained by a least squares curve fitting. However, due to the scatter within the individual data sets, two or more curves could intersect or converge. To prevent this, a model is constructed by coupling a model estimating Peak Ground Acceleration from earthquake parameters, to a model relating PGA to MMI, which is valid for the entire country. The models selected are the equation of Boroschek and Contreras, which was constructed from data of the Mw 8.8, 2010 Maule earthquake [4] and the equations from Wald et al. (1999) [5]. However, the equations derived by Wald are based on Californian data. Hence, a new MMI-PGA model is constructed from the Chilean data and compared against the others.

As a result, a set of non-intersecting curves relating hypocentral distance to magnitude for each MMI level are obtained. These curves are validated using additional data, which comprise events occurred between November 2014 and October 2015. These include the Mw 8.3 earthquake that took place on September 16th.

### 2.2 Tsunami scenario selection and propagation

The main objective of this work is to link the MMI with the level of alert of a tsunami by means of Mw-Δ-Alert Level curves. Here, Alert is meant as the hazard level as defined by SHOA at each location, it is evaluated based on maximum expected height of a tsunami triggered by an earthquake of moment magnitude Mw at a distance Δ from the location of interest.

The current classification of tsunamis according to their expected wave height is ‘Major’ Tsunami for heights of 3 m or higher, ‘Intermediate’, for heights between 1 and 3 m, ‘Minor’, between 0.3 and 1 m, and ‘Instrumental’ for lower than 30 cm.

Unfortunately, there are not enough tsunami height data available to construct these curves because SHOA has historic data of measurements made for only nine tsunamis that took place between 1971 and 2015, and many of these have only sparse latitudinal coverage. In addition, given that tsunamis have a high local variability, an alternative is required to fill this observational gap. Here, numerical modeling of tsunamis is used in order to solve this problem.

First, a set of earthquake scenarios is selected as to have a uniform coverage both in terms of earthquake magnitudes and spatial extension. Considering that prior experience suggests that small earthquakes (< Mw 7.0) only trigger instrumental tsunamis, and that larger earthquakes trigger large tsunamis, we first focus on the range of events for which tsunami occurrence and hazard level is less certain. This means events in the range between Mw 7.5 and 8.5, and depths between 15 and 35 km. Depth, dip, and strike are given by the shape of the trench, so deeper hypocenters imply earthquakes further inland. The scenarios were taken from an existing catalog, which comprises a total of 3056 scenarios of different characteristics and number of sub faults [6].

These scenarios are distributed uniformly along the coast with a separation of two degrees of latitude. A selection of points of interest (POIs) located around cities are used to estimate the hazard, through the computation of the tsunami time series associated to each event simulated. The POIs coincide with existing tide gauges, and with an array of points located in 50 m depth. The tsunami propagation model *EasyWave* [7] is used to estimate the time series at the different POIs. *EasyWave* solves the tsunami propagation by using *Linear Shallow Water Equations* and performs these calculations through the TUNAMI-F1 algorithm [8]. The coastal tsunami height is determined by using Green's Law to compute the corresponding height at each POI after the equations become invalid, i.e. nearshore. The software uses as initial conditions the deformations on the surface calculated from the earthquake characteristics, using the model by Okada [9]. EasyWave was chosen due to its fast computation time. Nevertheless, validation tests using COMCOT showed that model selection had a negligible impact on the results.

## 2.3 MMI-Δ-Tsunami Level curves

Tsunami time series are reduced to the maximum amplitude value, and thus are associated to a hazard level. A scatter plot relating hazard level against distance for each city is constructed. Due to the scatter, a best-fit line is created by selecting one point from each magnitude and tsunami category that fulfills the following conditions: i) produces a major tsunami, ii) is located at the longest distance among the array of points of the same magnitude and tsunami level, iii) is not an outlier.

One additional quality control is imposed, aimed to prevent intersecting curves whilst retaining a good level of detection. To estimate the latter, percentages of false detections were estimated for the following cases:

i) Major events falling under the major-intermediate line over the total number of major events, indicating underestimation.

ii) Intermediate over the major-intermediate line, indicating overestimation.

iii) Intermediate under the intermediate-minor line.

iv) Minor over the intermediate-minor line.

An objective function (Eq. 1) is defined with these parameters.

$$f = \frac{\sum_{i=1}^{4} q_i P_i d_i}{\sum_{i=1}^{4} d_i} \qquad (1)$$

where $q_i$ is the weight associated with each percentage, $P_i$ is the percentage of data out of bounds in each category, and $d_i$ is the number of events in each one of the four categories. It has been favored that major values fell into the proper category by giving that part of the function a higher weight.

To minimize this function, a weighted average function (Eq. 2) for the slopes of the first two separation lines is defined:

$$avg_{slope} = w_1 s_1 + w_2 s_2 \qquad (2)$$

where $w_i$ is the weight associated to each slope, and $s_i$ are the initial slopes.

With this, different weights are tested to obtain the best option. Also, the position coefficient of each curve is also iterated, so their position changes with a change in slope. A final restriction imposed is that the separation between the lines exceeds a fixed minimum. In most of the cases this difference is equal to 0.5 magnitude units, with the objective of keeping the lines sufficiently separated. With these steps, the dividing lines with minimum out of bound percentages for each category are obtained. It is verified that the percentages of data out of bounds do not exceed 30% for the curve separating major from intermediate events, and not more than 40% for intermediate-minor and minor-instrumental data.

## 3. Results

### 3.1 MMI-Δ-Mw curves

2417 earthquake events (classified by MMI, as shown in Table 1) are used to construct the best fit line for each MMI. Sample results are shown in Fig. 1, where it can be seen that data show a considerable scatter, yet indicate a clear trend. Data above the line suggest the underestimation of their MMI by the report and conversely for the data below the line.

Table 1 – Number of reports collected for events occurred in the period 2011-2014, by MMI

| MMI | II | III | IV | V | VI | VII | VIII | Total |
|---|---|---|---|---|---|---|---|---|
| # of Reports | 666 | 948 | 550 | 194 | 43 | 7 | 9 | 2417 |

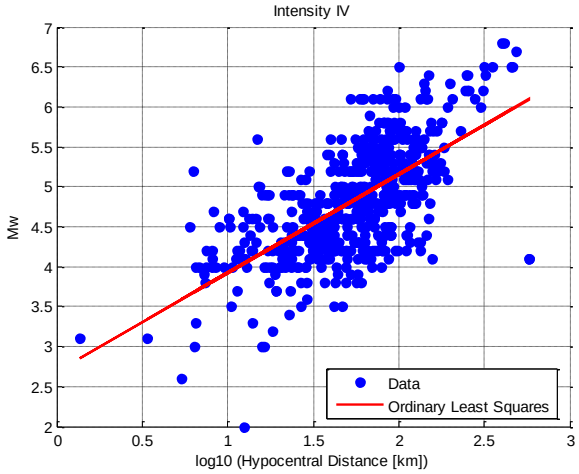


Fig. 1 – Example of best fit line and scatter of reported data, MMI IV

As a result of the scatter, and due to possible misreporting, lines might intersect. The problem is more persistent at higher intensities due the smaller number of events. Hence, to reduce the effect of misreporting and subjectivity, a different approach has been tested. Here, the procedure used by Wald et al. is followed, upon which the MMI is estimated from the geometric mean of the peak horizontal ground acceleration.

The results are Eq. 3 and Eq.4 (also shown on Fig. 2).

$$MMI = 5.0952 \log PGA - 1.3417; MMI < IV \quad (3)$$

$$MMI = 2.9979 \log PGA + 0.7792; MMI \geq IV \quad (4)$$

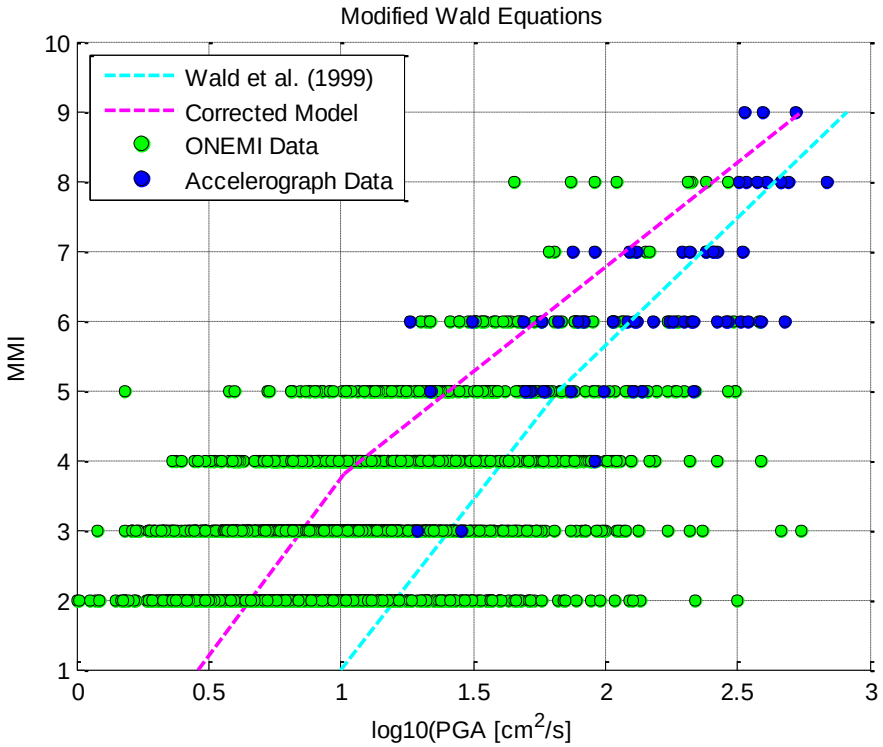


Fig. 2 – Corrected Wald equations based on original data (intensity vs log PGA graph), the scattered data are the reports collected both from ONEMI and accelerograph data (available through the site *terremotos.uchile.cl*)

These adjust better to the reports, despite the high dispersion. Also, local behavior is being added as a factor here, so they become more representative of Chile-specific situations.

At this point, we have, schematically

$$\mathrm{MMI} = \mathrm{f}(\mathrm{PGA}) \tag{5}$$

While, at the same time, after checking Boroschek & Contreras (2012):

$$PGA = g(\{Earthquake\ Parameters\}) \tag{6}$$

The earthquake parameters used by this equations are magnitude, depth, minimum distance to the hypocenter and dip and strike angles.

By combining Eq. 5 with Eq. 6 it is possible to estimate the MMI based solely on the earthquake parameters needed. This is:

$$MMI = f(g(\{E.P.\})) \tag{7}$$

It is important to note that in solving Eq. 7, a representative depth of 35 km has been used. To construct the final curves to be used, Eq. 7 is solved for MMI separately, and by iterating over a range of distances (up to 1000 km), enough values of moment magnitude are obtained to generate the corresponding curve for each intensity. The final results are shown in Fig. 3 (left), where it can be seen that curves do not intersect. This chart suggests that for a given report, consisting of a certain MMI value at a location, if the hypocenter is located at a distance Δ, the expected Mw magnitude could be calculated.

In order to validate these curves, a different data set is used (events from January to October 2015, Table 2). After applying the same filtering as the initial data, a total of 268 events (1031 reports) are considered. The validation shows that both the lines and the depth selected are representative. An example is shown in Fig. 3 (right).

Table 2 – Reports generated between November 2014 and October 2015

| MMI | II | III | IV | V | VI | VII | VIII | Total |
|---|---|---|---|---|---|---|---|---|
| # of Reports | 159 | 475 | 258 | 89 | 41 | 6 | 3 | 1031 |

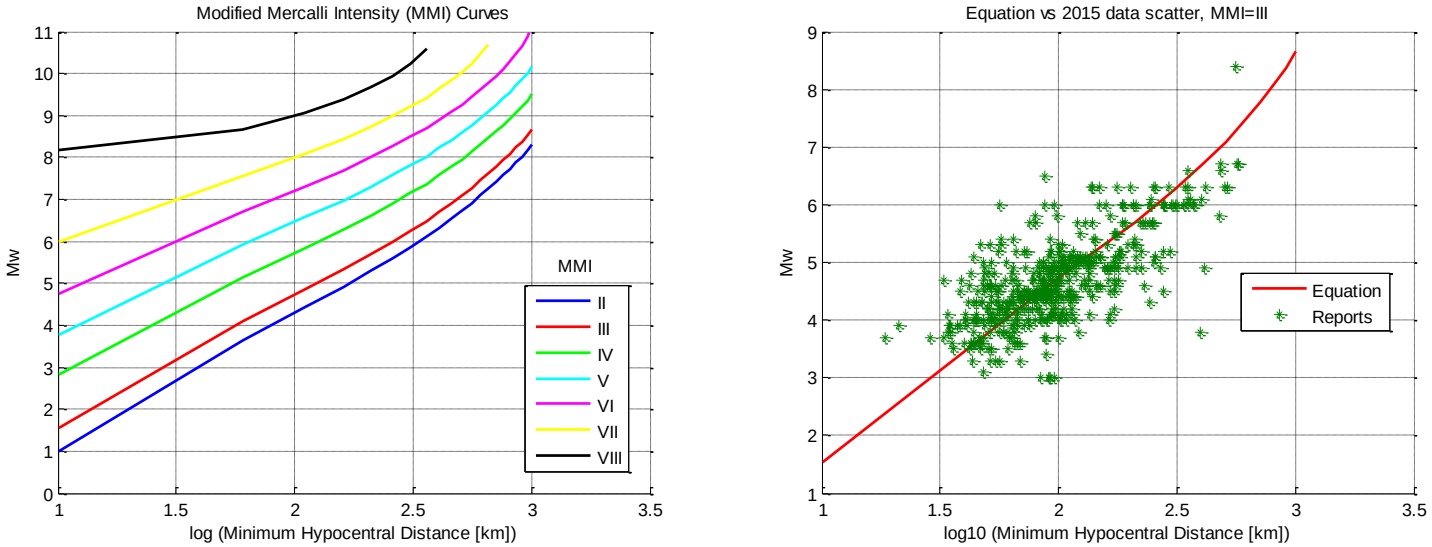


Fig. 3 (left) – Final MMI-Δ-Mw curves, for MMI between II and VIII; (right) - Example of validation of MMI-Δ-Mw curves by using new collected data (MMI = III)

## 3.2 Mw-Δ-Tsunami Level curves

As described in section 2.2, 136 tsunami scenarios are selected by distributing them uniformly along the Chilean coast, while also concentrating them around nine selected cities. From these, 36 correspond to Mw 7.5 earthquakes, 68 to Mw 8.0, and 32 to Mw 8.5. In Table 3, the location of the cities is presented along the number of observation points (tide gauges) from which the maximum wave heights are estimated.

Table 3 – Location of the 9 cities considered for the Hazard Assessment Charts. For each city, POIs consider the actual tide gauge plus synthetic ones.

| City | Latitude | Longitude | POIs |
|---|---|---|---|
| Arica | -18.475 | -70.314 | 4 |
| Iquique | -20.217 | -70.167 | 7 |
| Antofagasta | -23.633 | -70.400 | 11 |
| Coquimbo | -29.950 | -71.333 | 10 |
| Valparaíso | -33.067 | -71.633 | 10 |
| San Antonio | -33.600 | -71.617 | 9 |
| Constitución | -35.333 | -72.417 | 7 |
| Talcahuano | -36.717 | -73.117 | 6 |
| Ancud | -41.867 | -73.833 | 7 |

The maximum values from each of the time series generated are extracted, and for each city all these values are collected and classified according to the tsunami levels defined by SHOA, as described in section 2.2. The results of such assortment for each city are displayed in Table 4.

Table 4 – Distribution of results for each city

| Location | # of Results | Major (%) | Intermediate (%) | Minor (%) | Instrumental (%) |
|---|---|---|---|---|---|
| Arica | 544 | 9.38 | 21.51 | 33.46 | 35.65 |
| Iquique | 952 | 6.41 | 14.08 | 22.90 | 56.61 |
| Antofagasta | 1496 | 4.75 | 11.97 | 28.28 | 55.00 |
| Coquimbo | 1360 | 7.06 | 17.28 | 26.91 | 48.75 |
| Valparaíso | 1360 | 5.74 | 17.79 | 26.19 | 50.28 |
| San Antonio | 1224 | 6.13 | 19.44 | 26.39 | 48.04 |
| Constitución | 952 | 13.34 | 24.47 | 34.03 | 28.16 |
| Talcahuano | 816 | 13.48 | 27.21 | 31.25 | 28.06 |
| Ancud | 952 | 3.78 | 11.97 | 27.11 | 57.14 |

Table 4 shows that local effects are relevant, as the distributions of tsunami hazard vary from place to place significantly. For example, Talcahuano is very prone to large events (40.69% of the events result in intermediate or greater tsunamis), whereas Ancud is fairly protected (74.25% of minor or smaller tsunamis). A similar table with COMCOT data has been produced, obtaining no significant differences. These data are plotted for each city, depending on its hazard level and hypocentral distance.

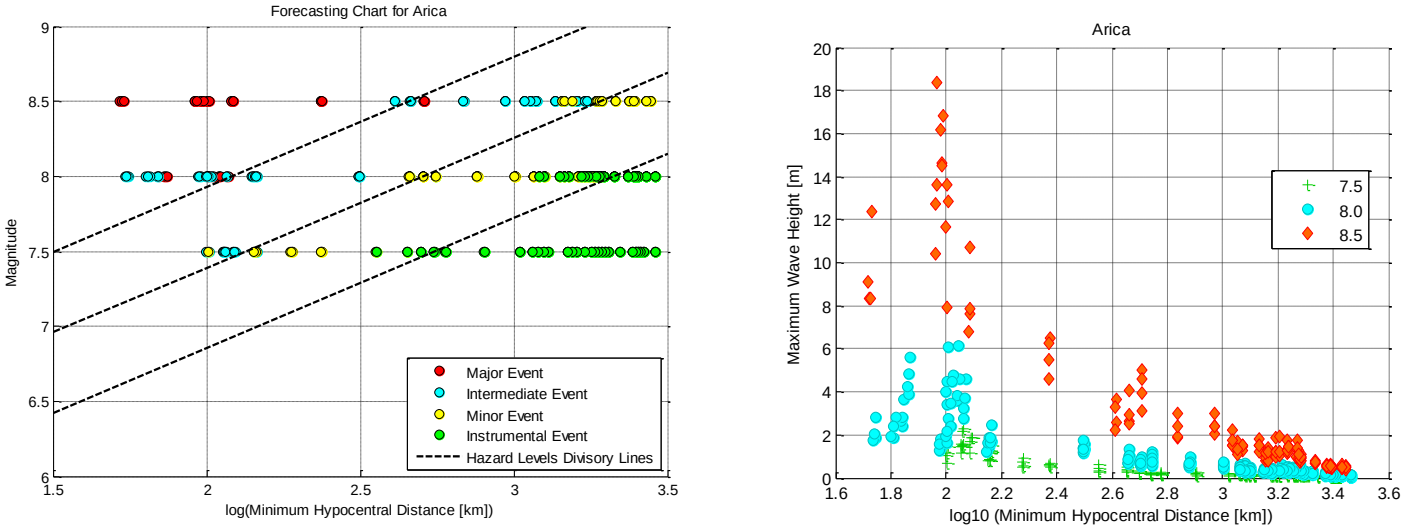


Fig. 4 (left) – Mw vs log-distance graph for Arica, with events classified by tsunami level and the lines described in Table 5; (right) – Maximum wave height vs log-distance graph for Arica (for simulated events), with events classified by Magnitude

In Fig. 4 (left) it is appreciable the relatively clear separation between each tsunami category, for the city of Arica. Fig. 4 (right), shows that the larger magnitude events generate the highest waves closer to the POI, and

a clear separation exists with lower magnitudes at close range, highlighting the possibility of discriminating between hazard levels and earthquake magnitude, by means of the Mw-Δ-Tsunami level separation curves.

The results of the discriminating curves are shown in Table 5, where data are classified by city. It can be seen that slope and intercepts values (position coefficients) could be associated with the potential vulnerability of a certain place against a tsunami. A smaller slope means that a major tsunami has a higher probability of occurring, due to a wider range of distances at which an earthquake can generate a tsunami of given characteristics. Also, a smaller position coefficient causes this same effect, because a lower intensity (or magnitude) might mean that there is still the latent possibility of a large tsunami coming, due again to a wider batch of scenarios able to generate these conditions.

Table 5 – Slopes and Position Coefficients of the dividing lines for each city

| City | Slope | Pos. Coeff. 1 | Pos. Coeff. 2 | Pos. Coeff 3 |
|---|---|---|---|---|
| Arica | 0.8654 | 6.1992 | 5.6625 | 5.1258 |
| Iquique | 0.7324 | 6.7730 | 6.2529 | 5.7285 |
| Antofagasta | 0.7943 | 6.6971 | 6.1964 | 5.6958 |
| Coquimbo | 0.7185 | 6.8335 | 6.3251 | 5.8187 |
| Valparaíso | 0.7103 | 6.9844 | 6.4634 | 5.9423 |
| San Antonio | 0.8310 | 6.8375 | 6.2996 | 5.7618 |
| Constitución | 0.5737 | 6.9869 | 6.4690 | 5.9510 |
| Talcahuano | 0.6319 | 6.7436 | 6.2956 | 5.8476 |
| Ancud | 1.0232 | 6.4776 | 5.6910 | 4.9045 |

By comparing these results to the preliminary distribution of the simulated tsunamis it can be noted that those places marked as more prone to higher tsunamis (Constitución, Talcahuano, Table 4), have the lowest slopes among the nine cities considered. At the same time, Arica, which is third in terms of the percentage of intermediate plus major events (30.89%), has the lowest position coefficients of all cities for its three position coefficients despite presenting the second highest slope of the group. This can be interpreted to Talcahuano and Constitución being prone to be affected by tsunamis originating at several places along the coast, whereas Arica can be very sensitive to small magnitude earthquakes nearby.

On the other hand, the most protected location is Ancud, which has only a 15.75% of major or intermediate tsunamis. It presents the highest slope but has the lowest position coefficients of the set. This suggests that Ancud is relatively insensitive to far field tsunamis, but can be affected by local ones.

## 4. Discussion

One of the main goals of this work is to improve the assessment capability. To test this, an example is used with real data reported and registered after the earthquake and tsunami occurred on April 1st, 2014. The parameters which define the earthquake are given in Table 6.

Table 6 – 1st April 2014 Earthquake parameters

| **Parameter** | **Mw** | **Latitude [°]** | **Longitude [°]** | **Depth [km]** | **Dip Angle [°]** | **Strike Angle [°]** |
|---|---|---|---|---|---|---|
| **Value** | 8.1 | -19.70 | -70.81 | 21.6 | 15 | 355 |

As for this example, depth, dip, strike, and the coordinates of the epicenter are assumed as known. These are used in order to estimate the minimum hypocentral distance. The location and reports of the places that perceived and reported the earthquake are shown in Table 7. This information has been taken from the CSN website (*sismologia.cl*).

Table 7 – Intensity reports for the Iquique earthquake

| Location | Lat. [°] | Long. [°] | MMI | Location | Lat. [°] | Long. [°] | MMI |
|---|---|---|---|---|---|---|---|
| Arica | -18.475 | -70.314 | VIII | Tocopilla | -22.067 | -70.200 | VI |
| Codpa | -18.833 | -69.744 | VIII | María Elena | -22.035 | -69.667 | V |
| Cuya | -19.160 | -70.179 | VIII | Calama | -22.467 | -68.917 | VI |
| Iquique | -20.217 | -70.167 | VII | Sierra Gorda | -22.883 | -69.317 | IV |
| Alto Hospicio | -20.268 | -70.105 | VII | San Pedro de Atacama | -22.917 | -68.217 | VI |
| Ollagüe | -21.217 | -68.267 | V | Mejillones | -23.100 | -70.450 | V |
| Quillagua | -21.660 | -69.535 | VI | Antofagasta | -23.633 | -70.400 | III |

The Mw-Δ-MMI chart is used by locating these reports using the distance calculated, and the intensity provided. These results are shown in Fig. 6. In this figure, the crosses represent the evaluation of the MMI reports on their corresponding intensity curve, which allow estimating a preliminary magnitude value.

It can be seen that the magnitudes evaluated through this procedure range within the values of approximately Mw 6.4 and 8.9, which is too broad. However, it is important to note as well that the low-intensity reports are the worst at predicting the magnitude of the earthquake, while intensities over VI are preferred. In consequence, if the reports for intensities lower than VI are not considered, the range of predicted magnitudes is reduced to values between 7.2 and 8.9 (indicated with circles in Fig. 5, left). It is thus suggested that the hazard level evaluation only considers those magnitude estimations that are allocated between the 25$^{th}$ and 75$^{th}$ percentile of the data reported as VI of higher, which permit to have a more bounded range. By applying this condition, the estimated range of possible magnitudes is reduced to 7.2 up to 8.3, containing the actual magnitude of that earthquake (Mw 8.1).

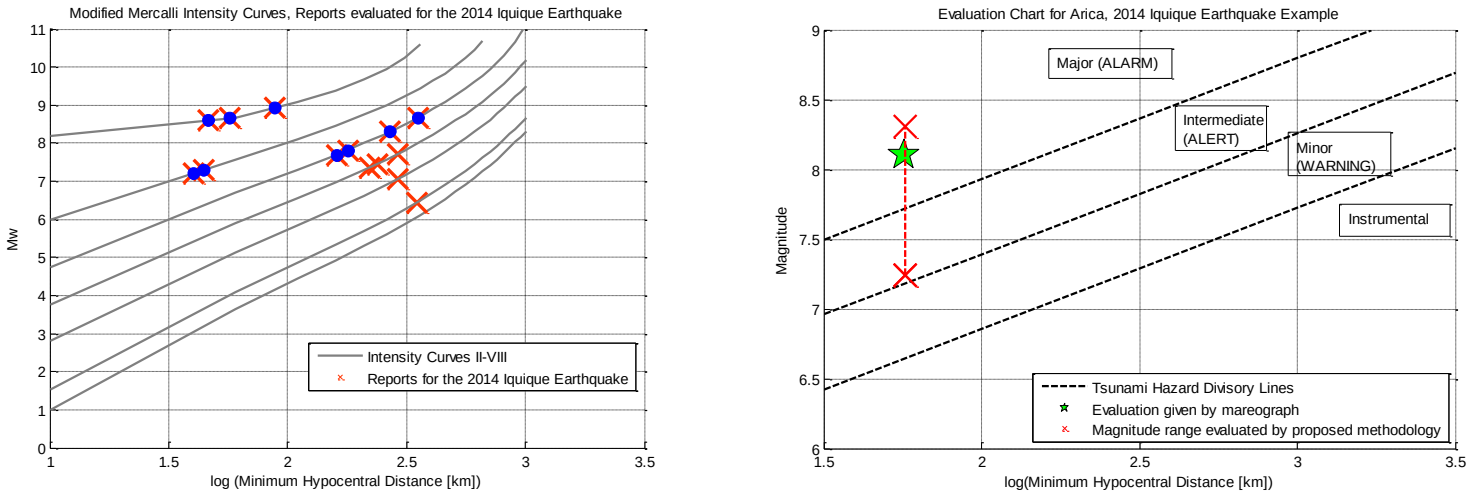


Fig. 5 (left)– Evaluation of the reports generated after the 2014 Iquique earthquake, evaluated in the MMI-Δ-Mw chart; (right)– Result of evaluating the TWC for Arica by using the proposed method. The star shows the evaluation of the real hazard for the city obtained via the tide gauge.

By combining this range with the corresponding distance to the hypocenter, the tsunami hazard levels which are more prone to occurring are obtained. This range is shown with crosses in Fig. 5 (right), indicating either intermediate or major tsunami. Now, in order to check if the evaluation is appropriate enough, it is checked if the evaluation of the data from the corresponding tide gauge falls within this range [10]. By entering directly to Fig. 5 (right) with the magnitude of the earthquake and the distance from the tide gauge to the hypocenter, the star in this same chart is obtained, indicating the occurrence of a major tsunami. This shows that the range given by evaluating the MMI reports encompasses the direct evaluation of the location of the tide gauge. This means that the forecast in this case is adequate enough, and it would have permitted to develop the proper evacuation protocols for Arica.

Table 8 – Levels of overestimation in the TFCs for each city, for three different earthquakes. (N/D: No Data Available, due to no registered data or failure of the tide gauge during the earthquake, in the case of San Antonio and Constitución in 2010)

| City | Maule 2010 | Iquique 2014 | Illapel 2015 |
|---|---|---|---|
| Arica | 0 | 1 | 0 |
| Iquique | 1 | 1 | 1 |
| Antofagasta | 1 | 1 | 0 |
| Coquimbo | 1 | 1 | 0 |
| Valparaíso | 1 | 0 | 0 |
| San Antonio | N/D | 0 | 0 |
| Constitución | N/D | 0 | 0 |
| Talcahuano | 1 | 0 | 0 |
| Ancud | N/D | N/D | N/D |

It is important to note as well that the maximum height registered by the tide gauge is not used directly in terms of the evaluation of these charts. However, this can be used to check if the hazard levels are coherent between both measurements. In this case, the maximum wave height registered by the tide gauge is 1.95 m, which implies intermediate tsunami, meaning that the chart has overestimated the hazard level by one. This situation repeats for the majority of the cases analyzed, as presented in Table 8. The table shows that within the cases studied there are no situations in which an underestimation is presented. This is relevant because there is no risk of dismissing an evacuation procedure because the result of the evaluation indicates that a destructive tsunami will not occur. On the other hand, these overestimations are accepted due to the preliminary nature of the procedure presented. In other words, this means that it is preferred to cancel an evacuation procedure after more detailed information is gathered, than having to issue an evacuation alarm when it is too late.

## 5. Conclusions

The possibility of using Modified Mercalli Intensity curves to evaluate tsunami risk has been evaluated with satisfactory results that reduce the effect of its subjectivity. By overlapping the results of those curves with the increased tsunami events, charts for nine cities have been developed. From the proposed methodology, the results appear to be coherent with the increased hazard some places are known to have. As a future work, the proposed evaluation method needs to be checked thoroughly, even though it can be stated preliminarily that it tends to overestimate the hazard risk at most in one level. These results show that the perception of earthquakes in Chile behaves similarly to the curves generated, and suggest that the curves are appropriate to be used in the future instead of individual reports on their own, to evaluate the intensity in different locations.

## 6. Acknowledgements

We would like to thank the Chile-Japan Joint Project on Enhancement of Technology to Develop Tsunami Resilient Communities, sponsored by the Japan Science and Technology Agency (JST) and the Japan International Cooperation Agency (JICA) through its SATREPS initiative.

We would also like to express our gratitude to CONICYT, for financing the principal author of this paper in the context of the *Programa de Capital Humano Avanzado, Beca Magíster Nacional 2015 – N° 22150320.*

Finally, we wish to appreciate the assistance given by CIGIDEN, for financing the registration to this conference of the main author.

## 7. References

[1] Bernard E., Titov V., 2015. *Evolution of tsunami warning systems and products*. Phil. Trans. R. Soc. A 373, 20140371.

[2] Protocolo ONEMI-SHOA para evento de Tsunami en las costas de Chile.

[3] Papazachos B. C., Scordilis E. M., Panagiotopoulos D. G., Papazachos C. B., Karakaisis G. F., 2004. *Global Relations Between Seismic Fault Parameters and Moment Magnitude of Earthquakes*. Bulletin of the Geological Society of Greece vol. XXXVI, 2004.

[4] Boroschek R., Contreras V., 2012. *Strong Ground Motion from the 2010 Mw 8.8 Maule Chile Earthquake and Attenuation Relations for Chilean Subduction Zone Interface Earthquakes*. Proceedings of the International Symposium on Engineering Lessons Learned from the 2011 Great East Japan Earthquake, March 1-4, 2012, Tokyo, Japan

[5] Wald D., Quitoriano V., Heaton T., Kanamori H., 1999. *Relationships between Peak Ground Acceleration, Peak Ground Velocity, and Modified Mercalli Intensity in California. Earthquake Spectra*. August 1999, Vol. 15, No. 3, pp. 557-564.

[6] Riquelme S., Mocanu M., 2012. *Informe Técnico: Desarrollo de una base de datos de fuentes tsunamigénicas para Chile.* Proyecto SHOA-Universidad de Chile.

[7] Babeyko, A., 2012, *EasyWave: Fast Tsunami Simulation Tool for Early Warning*.

[8] IUGG/IOC Time Project. *IOC Manuals and Guides No. 35*. UNESCO 1997.

[9] Okada, Y., 1985. *Surface deformation due to shear and tensile faults in a half-space*. Bull. Seism. Soc. Am. 75, 1135-1154.

[10] Catalán, P. A., et al. (2015), *The 1 April 2014 Pisagua tsunami: Observations and modeling*, Geophys. Res. Lett., 42, doi: 10.1002/2015GL063333.